# Thermomechanical analysis induced by interrupted cutting of Ti6Al4V under several cooling strategies

P. Lequien *, G. Poulachon (1), J.C. Outeiro (2)

*Arts et Metiers, LaBoMaP Laboratory, UBFC, 71250 Cluny, France*

ARTICLE INFO

*Article history:*
Available online 19 April 2018

*Keywords:*
Cryogenic machining
Thermal effects
Interrupted cutting

ABSTRACT

Cryogenic machining has mainly investigated in continuous cutting. Therefore, there is a lack of knowledge on the application of this technology to interrupted cutting, such as in milling. This study aims to investigate the thermomechanical phenomena in interrupted cutting of Ti6Al4V alloy under cryogenic, flood cooling and dry conditions. Due to the complexity of the thermomechanical analysis in milling, a special designed experimental setup has been developed through interrupted turning tests. This work highlights the influence of cryogenic flow rate and cutting time/non-cutting ratio on tool temperature. The obtained results can be extrapolated to milling operation.

## 1. Introduction

Machining refractory alloys generate high localized temperatures due to their poor thermal conductivity, high friction coefficient and high sensitivity to strain and strain-rate. As a consequence, rapid tool wear and poor surface integrity is observed when machining such alloys [1–3]. Several coolant strategies and/or machining assistances, including cryogenic assisted machining and tool vibration, can be applied to reduce these problems [4,5]. Indeed, cryogenic assisted machining, where liquid nitrogen ($LN_2$) is projected to the cutting zone, can be an effective solution to reduce the temperature in machining such alloys [6].

Challenges of cryogenic assisted machining are numerous and the cutting process of refractory alloys should be improved [7,8]. However, this poor controlled technology of liquid nitrogen deliverer to the cutting zone does not permit to compare all scientific works on cryogenic assisted machining, due to the scatter in the applied cooling conditions. In general, scientific publications agree on the benefit of $LN_2$ cooling in tool wear reduction, but show a scatter in terms of thermal phenomena and workpiece's surface integrity [9,10].

Several strategies to supply $LN_2$ to the cutting zone can be found in the literature. It seems that the most efficient way is to deliver $LN_2$ on the tool rake and flank faces, simultaneously [7]. Moreover, the efficiency of the cooling process depends on all $LN_2$ projection parameters, such as: flow rate, liquid/gas phase ratio, jet orientation and divergence, distance between the nozzle and the cutting zone. The convective heat transfer coefficient is a good indicator of this efficiency. Different convective heat transfer coefficients can be found in the literature without specifying all the $LN_2$ projection parameters [11,12]. The understanding of the physical phenomena during $LN_2$ projection is important to improve the efficiency of cryogenic assisted machining. $LN_2$ routing from the ranger to the nozzle has to be improved as well, in order to maximize the liquid/gas phase ratio at nozzle exit and to minimize the $LN_2$ loses [13].

Most of works on cryogenic assisted machining found in the literature are related with continuous cutting and very few of them deal with interrupted cutting [14]. In this case, many unknowns exist, including: the proper $LN_2$ routing system, the optimal $LN_2$ projection strategy and parameters, and their consequences in the cutting forces, tool wear and surface integrity.

The objective of the present work is to analyse the influence of $LN_2$ cooling on the tool temperatures and cutting forces in interrupted cutting of Ti6Al4V alloy, and compare it with dry and flood coolant conditions. In the case of milling, it's difficult to deliver the $LN_2$ through spindles and rotating tools, which requires particular precautions. Therefore, it seems to be easier to propose a thermomechanical analysis of interrupted cutting under cryogenic cooling conditions, using a fixed cutting tool and a workpiece shape. For such reason, interrupted turning tests are used to reproduce the milling operation.

## 2. Experimental set-up and parameters

Fig. 1 shows the experimental setup used in turning tests of Ti6Al4V alloy, using CNMG 120408 type uncoated cemented carbide cutting inserts. In order to deliver $LN_2$ at the cutting zone, a phase separator was used between the ranger and the tool holder. This phase separator is controlled using information from delivering temperature (at the phase separator exit) and $LN_2$ level

* Corresponding author.
*E-mail address:* pierre.lequien@ensam.eu (P. Lequien).

measurements. To ensure steady-state flow conditions, the $LN_2$ system (from the ranger to the nozzle) was cooled down before performing any test.

$LN_2$ is projected into both tool flank and rake faces using nozzles of different diameters. Variable nozzle diameters (1–3 mm) are used to spray $LN_2$ into the tool rake face, while a fixed nozzle diameter of 1.2 mm is used at tool flank face. The pressure was fixed at 2 bars. The average flow rate is determined by measuring the mass difference in the $LN_2$ ranger during the machining tests. These average flow rates are equal to 1.2, 1.9 and 2.5 l/min, corresponding to the nozzle diameters of 1, 2 and 3 mm, respectively.

Tool holder's internal channels for $LN_2$ delivering are previously optimized (by minimizing the angles through the flow), as well as the projection parameters (pressure, nozzle diameter, jet orientation and distance between the nozzle and the cutting zone), in order to maximize the convective heat transfer coefficient. In this case, $LN_2$ jet is oriented at $\alpha = 15°$ and $\beta = 10°$ in relation to the tool rake and flank faces, respectively (Fig. 1). The projection distance (d) is equal to 12 mm (Fig. 1).

A piezoelectric dynamometric (Kistler, model 9121) is used to measure the forces, while embedded thermocouples ($TC_i$) in the tool were used to measure the tool temperatures. Three thermocouples are placed in a hole having 0.5 mm of diameter and located at 1 mm beneath the tool rake face. The thermocouples ($TC_1$, $TC_2$ and $TC_3$ in Fig. 1) are placed in strategic positions in the tool, in order to compare the cooling influence on the tool temperature distribution.

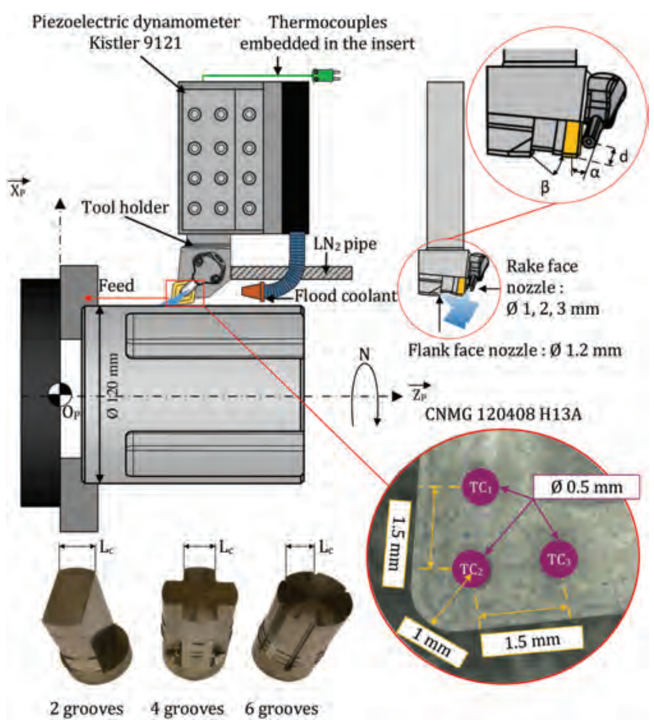


**Fig. 1.** Experimental set-up for interrupted turning tests of Ti6Al4V alloy.

Two kinds of experimental tests were carried out: (1) longitudinal turning tests over cylindrical workpieces, and (2) interrupted turning tests were performed on grooved workpieces (Fig. 1), to emulate a milling operation with a 40 mm milling cutter diameter ($D$). All of the samples have the same tool-workpiece engagement length ($L_c$) value of 31.4 mm, which is calculated by Eq. (1).

$$L_c = \frac{D}{2} \times arccos\left(1 - 2 \times \frac{a_e}{D}\right) \quad (1)$$

$a_e$ is the radial depth of cut which is considered to be 0.5.$D$. Three workpieces of 120 mm diameter having 2, 4 or 6 grooves are designed, which are representative of the different frequencies of tool-workpiece engagement in milling operation (i.e. 5.3 $H_z$ at $v_c$ = 30 m/min and 9.7 Hz at $v_c$ = 55 m/min with a 4 grooves workpiece). Cutting and non-cutting length ratio are 16%, 33% and 50% for 2, 4 and 6 grooves, respectively.

## 3. Results

### 3.1. Longitudinal turning tests

Priory to establish the design of experiments (DoE) for the interrupted turning tests, the determination of the restricted range of cutting conditions ($v_c$, $f$ and $a_p$) for turning Ti6Al4V titanium alloy is mandatory. The minimum values of the cutting conditions can be determined by applying the methodology of minimal specific cutting forces ($K_c$) variation in function of the cutting conditions, according to the AFNOR standard NF E66-520-4-97. As an example, Fig. 2 shows the variation of $K_c$ in function of $f$, keeping constant $v_c$ and $a_p$. Applying the above-mentioned methodology, the minimum $f$ to be used in the interrupted turning tests should be 0.125 mm.

Fig. 2 also provides information about the influence of the cooling strategy on $K_c$. Firstly, depending on the lubrication strategy, three sets of $K_c$ curves can be identified, being flood coolant the current industrial reference for Ti6Al4V alloy machining. Secondly, for low $LN_2$ flow rates (1.2 l/min), which corresponds to near dry machining, the corresponding $K_c$ curves (set 1) are below the flood one. However, $K_c$ increases with the $LN_2$ flow rate (from 1.2 l/min, corresponding to set 1, to 1.9 l/min, corresponding to set 2). $K_c$ will increase even more when $LN_2$ is projected on both tool rake and flank faces, simultaneously (set 3). Therefore, the projection of $LN_2$ on tool flank face has a non-negligible effect on $K_c$. In total, $K_c$ increases 1.5 times from set 1 to set 3. This is due to the variation of the Ti6Al4V mechanical behavior and tribological conditions induced by the cooling strategies [7]. In particular, a possible increase of work material hardening while machining using high $LN_2$ flow rate.

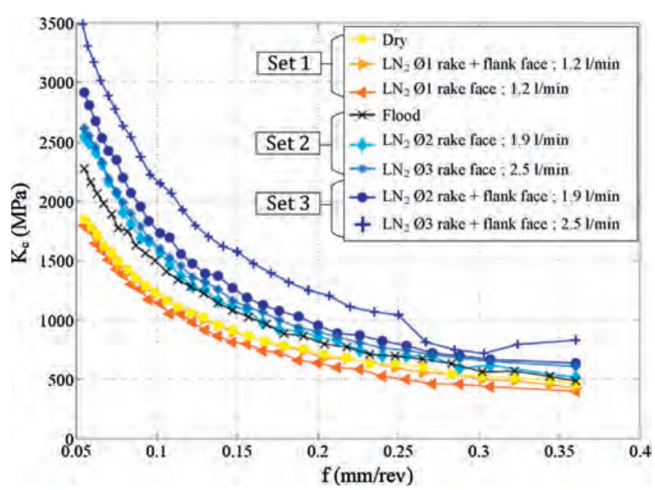


**Fig. 2.** Specific cutting forces ($K_c$) vs. feed (f) ($v_c$ = 55 m/min, $a_p$ = 1 mm).

### 3.2. Interrupted turning tests

Based on previous machining tests results, the following DoE for the interrupted turning is proposed. Four mains factors with two levels are chosen and presented in Table 1.

The $LN_2$ was projected simultaneously on both tool rake and flank faces. The measured parameters are the tool temperatures recorded by thermocouples ($T_{TC1}$, $T_{TC2}$ and $T_{TC3}$) and the cutting ($F_c$), feed ($F_f$) and penetration ($F_p$) forces.

Fig. 3 shows the results for a workpiece with 4 grooves. This figure points out an increase of the maximal cutting forces (Fig. 3a)

**Table 1**
Factors and levels used in the DoE of interrupted turning tests.

| Cooling conditions | Cutting conditions | |
|---|---|---|
| Dry | $v_c$ (m/min) | 30 and 55 |
| Flood (6% oil at 2 bars) | $f$ (mm) | 0.1 and 0.2 |
| $LN_2$ (rake and flank faces; nozzle Ø of 1 and 3 mm) | $a_p$ (mm) | 1 |
| Number of workpiece grooves | 2, 4 and 6 | |

and a decrease of the tool temperatures as the $LN_2$ flow rate increases (Fig. 3b). It appears that $F_p$ and $T_{TC2}$ are the most sensitive parameters to the cooling conditions. Therefore, further analysis will be focused only on the influence of $LN_2$ cooling on $F_p$ and $T_{TC2}$.

Fig. 4 aims to show the variation of $F_p$ and $T_{TC2}$ signals during an interrupted turning test. Fig. 4b shows the decrease of $T_{TC2}$ signal during machining. Temperature $T_{TC2}$ stabilization appears after 40 s of machining.

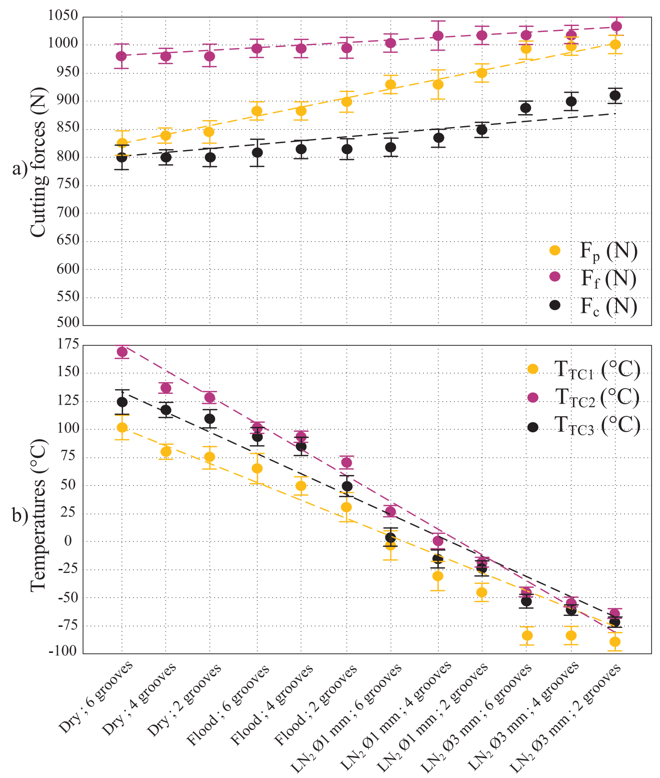


**Fig. 3.** Maximal forces (a) and temperatures (b) recorded during interrupted turning tests ($v_c$ = 55 m/min, $f$ = 0.2 mm/rev).

Fig. 4 zooms both $F_p$ and $T_{TC2}$ signals for one workpiece revolution. It is possible to point out a delay of 0.15 s between the sudden increase of $F_p$, when the tool become in contact with the workpiece, and the maximum generated $T_{TC2}$. The thermocouple response time is 0.05 s, which is negligible when compared to the observed delay between the force and temperature signals. So, this delay is probably due to the low thermal diffusivity of Ti6Al4V.

Fig. 5 represents the evolution of both $F_p$ and $T_{TC2}$ in function of the number of grooves. This figure shows that the number of grooves does not affect $F_p$, but it affects $T_{TC2}$. This temperature increases with the number of grooves. Increasing the number of grooves will increase the length of the tool cutting edge engaged in the workpiece and reduces the toolpath length between two consecutive workpiece tracks. Therefore, for the same cutting speed, increasing the number of grooves will increase the ratio between the cutting time and the non-cutting. Thus, more heat is generated by cutting and less time is available to cool down the tool before cutting the next track.

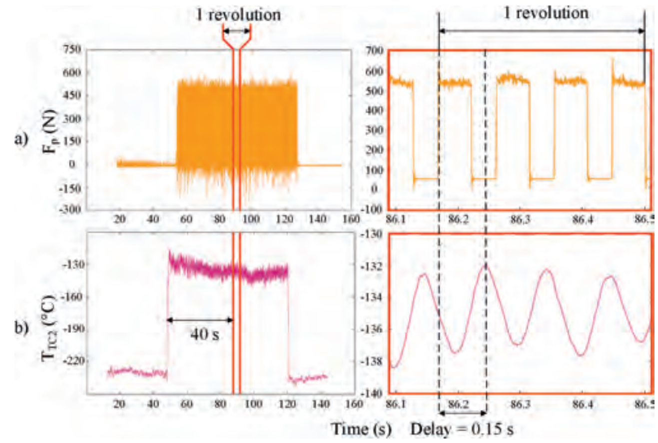


**Fig. 4.** Variation of $F_p$ and $T_{TC2}$ signals during an interrupted turning test (4?grooves workpiece, $v_c$ = 55 m/min, $f$ = 0.2 mm, $LN_2$ with Ø3 mm nozzle).

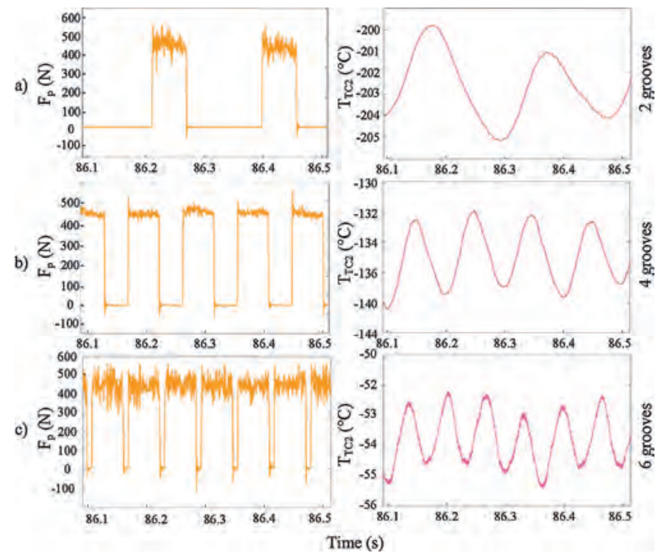


**Fig. 5.** Evolution of $F_p$ and $T_{TC2}$ as a function of workpiece grooves number ($v_c$ = 55 m/min, f = 0.2 mm/rev, $LN_2$ with Ø3 mm nozzle).

Fig. 6 shows the $T_{TC2}$ peak temperature in function of the number of grooves, for several cooling strategies (Fig. 6a) and cutting conditions (Fig. 6b). Fig. 6 put in evidence that this temperature always increases with the number of grooves,

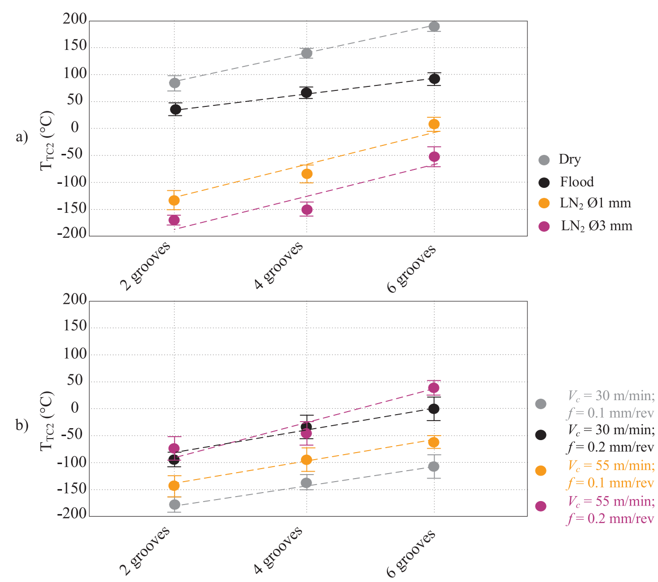


**Fig. 6.** $T_{TC2}$ peak temperature in function of grooves number for several: (a) cooling strategies ($v_c$ = 55 m/min, $f$ = 0.2 mm); and (b) cutting conditions ($LN_2$ with Ø3 mm nozzle).

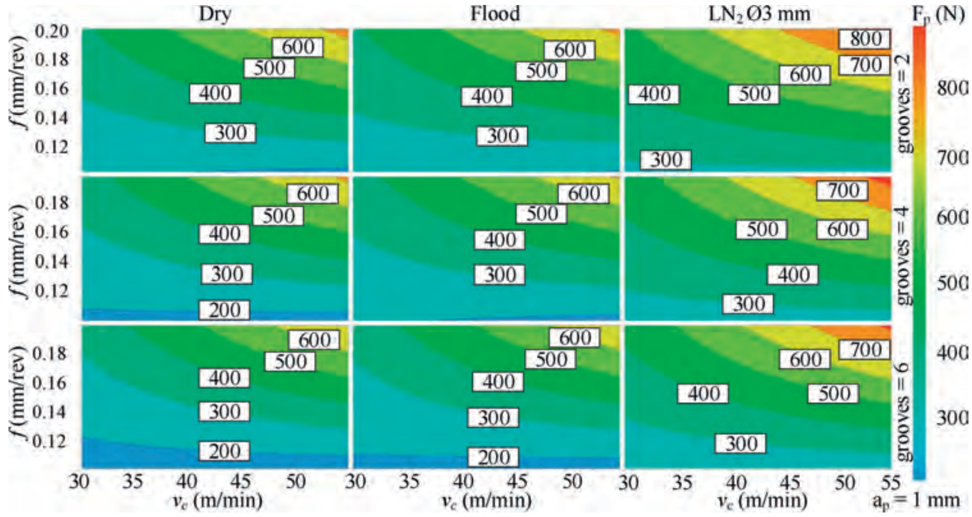


**Fig. 7.** 4D contour plot of $F_p$.

independently of the cooling strategy and cutting conditions. Moreover, lowest tool temperature is generated for $LN_2$ cooling at highest flow rate, and applying the lowest $v_c$ and $f$ values. This is due to smaller heat generated during cutting with the lowest $v_c$ and $f$ values, and the greater tool heat dissipation using the highest $LN_2$ flow rate.

In order to analyse all DoE results detailed in Table 1 and to present all the results in a single figure, a multilinear regression (MLR) analysis is applied as represented by the following general equation:

$$y_i = a_0 + a_1x_{i,1} + a_2x_{i,2} + \ldots + a_px_{i,p} + \varepsilon_p; (i = 1, \ldots n) \quad (2)$$

where $y_i$ is the total response, $x_{i,j}$ is the factor, $a_0$ the average value of the factor, $a_{i(i=1...4)}$ the polynomial coefficient, $a_{ij}.x_i.x_j$ are the interactions, and $\varepsilon_p$ the residual. This equation can be expressed through a matrix of the DoE factors:

$$\begin{bmatrix} T_{TCi} \\ F_i \end{bmatrix} = \begin{bmatrix} x_{11} & \ldots & x_{1p} \\ x_{i1} & x_{ij} & x_{ip} \\ x_{n1} & \ldots & x_{np} \end{bmatrix} \begin{bmatrix} \text{No. grooves} \\ V_c \\ f \end{bmatrix} + \begin{bmatrix} \varepsilon_1 \\ \varepsilon_i \\ \varepsilon_n \end{bmatrix} \quad (3)$$

Applying the ANOVA analysis, it is possible to evaluate the influence of each factor in $F_p$, for each cooling strategy. A 4D contour plot is used to represent the results of this statistical analysis, as shown in Fig. 7. This figure shows that the highest $F_p$ values are observed for $LN_2$ cooling, at high feeds and cutting speeds. This is possible due to an increase of work material hardening while machining using high $LN_2$ flow rate [7]. As already mentioned, the number of grooves does not affect $F_p$.

## 4. Conclusions

This paper presents thermomechanical analysis induced by dry, flood and $LN_2$ cooling conditions during machining of Ti6Al4V, using a special designed experimental set-up, combined with a statistical analysis of the results. Longitudinal turning tests showed that the specific cutting force is higher when $LN_2$ at high flow rate is projected on the tool rake and flank faces, simultaneously. The hypothesis of an increased work material hardening while machining using high $LN_2$ flow rate can be considered. In order to understand the influence of the cooling strategy in the thermomechanical phenomena in milling, simple interrupted turning tests were performed. These tests showed that the penetration force $F_p$ is the most affected parameter by the cooling strategy, when compared to the other components of the resultant force. A statistical analysis showed that the highest $F_p$ values are observed for LN2 cooling at high feeds and cutting speeds. Moreover, the number of workpiece grooves do not affect $F_p$, but it affects the tool temperature ($T_{TC2}$). This temperature always increases with the number of workpiece grooves, independently of the cooling strategy and cutting conditions. This is explained by an increase of the heat generated by cutting and less time to cool down the tool between tracks. These results can be extrapolated to milling operation.


## Acknowledgments

The authors are very grateful to Professor Joël Rech for his participation in this research work. The authors also would like to thank the French Funds for Industrial and Innovation (F2I) for their financial support.


## References


[1] Leyens C, Peters M, (Eds.) (2003), *Titanium and Titanium Alloys: Fundamentals and Applications*, Wiley-VCH, ISBN 3-527-30534-3.
[2] Rech J, Arrazola PJ, Claudin C, Courbon C, Pusavec F, Kopac J (2013) Characterisation of Friction and Heat Partition Coefficients at the Tool-work Material Interface in Cutting. *CIRP Annals—Manufacturing Technology* 62:79–82.
[3] M'Saoubi R, Outeiro JC, Chandrasekaran H, Dillon Jr OW, Jawahir IS (2008) A Review of Surface Integrity in Machining and Its Impact on Functional Performance and Life of Machined Products. *International Journal of Sustainable Manufacturing* 1:203–236.
[4] Bermingham MJ, Palanisamy S, Kent D, Dargusch MS (2012) A Comparison of Cryogenic and High Pressure Emulsion Cooling Technologies on Tool Life and Chip Morphology in Ti–6Al–4V Cutting. *Journal of Materials Processing Technology* 212:752–765.
[5] Paris H, Brissaud D, Gouskov A, Guibert N, Rech J (2008) Influence of the Ploughing Effect on the Dynamic Behaviour of the Self-vibratory Drilling Head. *CIRP Annals* 57:385–388.
[6] Hong SY, Markus I, Jeong W (2001) New Cooling Approach and Tool Life Improvement in Cryogenic Machining of Titanium Alloy Ti-6Al-4V. *International Journal of Machine Tools and Manufacture* 41:2245–2260.
[7] Jawahir IS, Attia H, Biermann D, Duflou J, Klocke F, Meyer D, Newman ST, Pusavec F, Putz M, Rech J, Schulze V, Umbrello D (2016) Cryogenic Manufacturing Processes. *CIRP Annals—Manufacturing Technology* 65:713–736.
[8] Yildiz Y, Nalbant M (2008) A Review of Cryogenic Cooling in Machining Processes. *International Journal of Machine Tools and Manufacture* 48:947–964.
[9] Courbon C, Kramar D, Krajnik P, Pusavec F, Rech J, Kopac J (2009) Investigation of Machining Performance in High-pressure Jet Assisted Turning of Inconel 718: An Experimental Study. *International Journal of Machine Tools and Manufacture* 49:1114–1125.
[10] Pusavec F, Krajnik P, Kopac J (2010) Transitioning to Sustainable Production—Part I: Application on Machining Technologies. *Journal of Cleaner Production* 18:174–184.
[11] Hriberšek M, Šajn V, Pušavec F, Rech J, Kopa J (2016) The Procedure of Solving the Inverse Problem for Determining Surface Heat Transfer Coefficient between Liquefied Nitrogen and Inconel 718 Workpiece in Cryogenic Machining. *Strojniški Vestnik—Journal of Mechanical Engineering* 62:331–339.
[12] Clausing AM (1990) Convective Heat Transfer Research Using a Cryogenic Environment. *Cryogenics* 30:335–340.
[13] Tahri C, Lequien P, Outeiro JC, Poulachon G (2017) CFD Simulation and Optimize of LN2 Flow Inside Channels Used for Cryogenic Machining: Application to Milling of Titanium Alloy Ti-6Al-4V. *Procedia CIRP* 58:584–589.
[14] Dhananchezian M, Pradeep Kumar M (2011) Cryogenic Turning of the Ti–6Al–4V Alloy with Modified Cutting Tool Inserts. *Cryogenics* 51:34–40.